

Convergence Results for Two Models of Interaction

by

Ryan Theisen

A Thesis Presented In Partial Fulfillment
of the Requirements for the Degree
Master of Arts

Approved August 2018 by the
Graduate Supervisory Committee:

Sebastien Motsch, Chair
Nicholas Lanchier
Eric Kostelich

ARIZONA STATE UNIVERSITY

December 2018

ABSTRACT

I investigate two models interacting agent systems: the first is motivated by the flocking and swarming behaviors in biological systems, while the second models opinion formation in social networks. In each setting, I define natural notions of convergence (to a “flock” and to a “consensus”, respectively), and study the convergence properties of each in the limit as $t \rightarrow \infty$. Specifically, I provide sufficient conditions for the convergence of both of the models, and conduct numerical experiments to study the resulting solutions.

ACKNOWLEDGMENTS

The work in section 2 on the model of flocking in three zones was done as part of ASU's MCTP program, together with Professor Motsch, Alex Reamy and Matthew Stokes. The work in section 3 on the consensus model was done together with Professor Motsch and Dylan Weber. Dylan Weber created figures 7-10 in section 3. I'm extremely grateful to Professor Motsch and the other amazing students I've been able to work with.

TABLE OF CONTENTS

Chapter	Page
LIST OF FIGURES	iv
1 INTRODUCTION	1
2 A MODEL OF FLOCKING IN THREE ZONES	1
2.1 Background	1
2.2 Three zone model	2
2.3 Convergence to a flock	2
2.4 Numerical investigation	5
2.5 Further work	7
3 A MODEL OF CONSENSUS FORMATION ON GRAPHS	9
3.1 Background	9
3.2 A stochastic approach to consensus formation	10
3.3 Poisson processes, interactions on graphs and the jump model	12
3.4 Convergence properties of the jump model	13
3.5 Strong convergence in the undirected case	16
3.6 Numerical investigation	19
3.7 Further work	22
4 CONCLUSION	22

LIST OF FIGURES

Figure		Page
1	Left: Illustration of the three-zone model. The model includes three types of behavior: attraction, alignment and repulsion. Right: attraction and repulsions are represented through the function V , alignment is described via ϕ	3
2	Attraction-repulsion V and alignment used for the simulations. In both cases, V diverges at infinity (i.e. satisfies (6))	6
3	Simulation of the three-zone model (1)-(2) with potential V and alignment function ϕ given by (8). Agents regroup on a disc of size $R \approx 1.8$ for any group sizes. Parameters: $\Delta t = .05$, total time $T = 100$	7
4	Simulation of the three-zone model (1)-(2) with potential V and alignment function ϕ given by (9). Agents regroup on a circle of size $R \approx .5$. Parameters: $\Delta t = .05$, total time $T = 100$	8
5	Evolution of the energy \mathcal{E} for the solutions depicted in figures 3 and 4. The energy is always decaying but also oscillates between fast and slow decays. These oscillations can be explained by the successive contraction-expansion of the spatial configuration. The decay of the energy is faster when the agents are closer to each other.	8
6	Summary of the results from theorems 3.1 and 3.2.	11
7	Illustration of the deterministic model with 2 strongly connected isolated components. Nodes in the top left component are initialized with opinion -1, whereas nodes in the bottom right component are initialized with opinion 1. Nodes in the center component are initialized with opinion 0.	19
8	Illustration of the averaging effect from the deterministic consensus model with 2 strongly connected isolated components after $t=1000$ periods. By theorem 3.2, the model converges, though not to a consensus, as there is more than one isolated strongly connected component.	20

9	Illustration of the initial setup of the stochastic model with $s_i \in \{-1, 1\}$. The nodes in the bottom right connected component are initialized to have opinion 1, whereas the nodes in the top left connected component are initialized to have opinion -1. The nodes in the center component are initialized randomly with opinion -1 or 1.	20
10	Stochastic consensus model after running the simulation for $t=1000$ periods. We see that the isolated components remain unchanged, and that the center component fails to reach consensus. Note that nodes more connected to the bottom right tend to have opinion 1, whereas nodes more connected to the top left component tend to have opinion -1.	21
11	Illustration of the decay of variance of opinions as given by theorem 3.10, with variance averaged over 10, 50, and 500 simulations.	21

1 Introduction

In this thesis, we explore two different models of interaction between N agents. The first is an extension of the well-studied Cucker-Smale model of flocking and swarming, in which agents interact according to three forces: attraction, repulsion, and alignment of velocity. Because of these three types of interaction, we call the model the ‘three-zone model’ of flocking. In the context of this model, we define a natural notion of convergence to a ‘flock’, and derive a sufficient condition for the dynamics to converge.

The second model studied in this thesis models the propagation of opinions or beliefs in a social network. We model each agent’s opinion as a scalar $s \in \mathbb{R}$, and define a *consensus* as a state in which all agents converge to a common opinion. In this model, the extent to which agents influence one another is determined by their configuration on a graph G . We show that a sufficient condition can be derived guaranteeing convergence of the system to consensus using only properties of the graph G .

Finally, we conduct numerical investigations for each model, and suggest potential future work.

2 A Model of Flocking in Three Zones

2.1 Background

Flocking behavior is an intriguing phenomenon observed in nature. It remains an open question how birds or fish are able to organize on several scales to form a coherent motion. Modeling has proved to be crucial in highlighting how such complex behaviors can be generated from simple interaction rules. Among the different models proposed, the three-zone model has been particularly popular in biology ([4],[8],[10]). In the three-zone model, agents representing birds or fish engage in three types of interactions: repulsion, alignment, and attraction, depending on whether their neighbor is at a short, intermediate, or long distance, respectively. The goal of this section is to provide sufficient conditions for the convergence of such a system towards a flock, which occurs when all agents approach a common velocity.

Analytical studies of flocking dynamics have mainly been inspired by the seminal work of Cucker and Smale ([5],[6]). In their research, they studied a simplified version of the so-called Vicsek model where only the alignment force between agents is considered. They proved rigorously the convergence of the dynamics to a flock, given the condition that the alignment force is sufficiently strong. This work has been followed by many generalizations and improvements ([9],[11]).

One key element to prove the convergence of the Cucker-Smale model to a flock is the decay of the kinetic energy of the system due to the alignment rule, which acts as a source of friction. In the present manuscript, the dynamics combine both attraction-repulsion and alignment, therefore we have to define the energy of the system as the sum of its kinetic energy and potential energy. The attraction-repulsion term does not modify the total energy since it obeys Hamiltonian dynamics, and hence conserves energy. However, the alignment term causes the kinetic energy and consequently the total energy of the system to decay with respect to time. As a result, if the attraction-repulsion force is such that the particle configuration remains spatially bounded, the influence of the alignment term will guarantee the system converges to a flock. Notice that we cannot draw any conclusions about the spatial organization of the flock, but many analytic and numerical

studies have been conducted on this problem.

So far, the sufficient condition for flocking requires that the attraction term is given by a confinement potential. However, this condition can be weakened by incorporating the effect of the alignment in the non-spatial dispersion of the agents. Here, the effects of attraction and alignment are treated separately. Using commutator techniques, it might be possible to improve the sufficient condition for flocking and/or to find a joint condition on the strength of attraction and alignment at large distances. Other perspectives will be to extend the proof for other types of interactions, such as non-symmetric interactions ([7],[9]), or using the so-called topological distance ([2],[3]).

The section is organized as followed: in section 2.2, we introduce the three-zone model for agent-based dynamics. We prove the main result by finding a sufficient condition for the emergence of a flock in section 2.3 and give several numerical illustrations in section 2.4.

2.2 Three zone model

We consider the three-zone model, which describes moving according to three rules of interaction: repulsion (at a short distance), alignment, and attraction (at long distance). A schematic representation of the model is given in figure 1. Each agent i is represented by a vector position \mathbf{x}_i and a velocity \mathbf{v}_i both belonging to \mathbb{R}^d (with $d = 2$ or 3). The evolution of the N agents is governed by the following system:

$$\dot{\mathbf{x}}_i = \mathbf{v}_i \tag{1}$$

$$\dot{\mathbf{v}}_i = \frac{1}{N} \sum_{j=1}^N \phi_{ij}(\mathbf{v}_j - \mathbf{v}_i) - \frac{1}{N} \sum_{j \neq i} \nabla_{\mathbf{x}_i} V(|\mathbf{x}_j - \mathbf{x}_i|) \tag{2}$$

Here, $\phi_{ij} = \phi(|\mathbf{x}_j - \mathbf{x}_i|)$ represents the strength of the alignment between agents i and j . We suppose that the function ϕ is strictly positive. Similarly, $\nabla_{\mathbf{x}_i} V(|\mathbf{x}_j - \mathbf{x}_i|)$ represents the attraction or repulsion of agent j on i . Indeed, developing the gradient gives:

$$-\nabla_{\mathbf{x}_i} V(|\mathbf{x}_j - \mathbf{x}_i|) = V'(|\mathbf{x}_j - \mathbf{x}_i|) \frac{\mathbf{x}_j - \mathbf{x}_i}{|\mathbf{x}_j - \mathbf{x}_i|}.$$

Thus, agent i is attracted to agent j if $V' > 0$ and repulsed if $V' < 0$. In figure 1, we illustrate two possible choices for ϕ and V .

2.3 Convergence to a flock

The goal of this section is to prove conditions guaranteeing that the three-zone model (1)(2) converges to a *flock*.

Definition 2.1. *We say that a configuration $\{\mathbf{x}_i, \mathbf{v}_i\}_i$ converges to a flock if the following are satisfied:*

1. *There exists \mathbf{v}_∞ such that $\mathbf{v}_i \rightarrow \mathbf{v}_\infty$ as $t \rightarrow \infty$ for all $i = 1, \dots, N$.*
2. *There exists M such that $|\mathbf{x}_j - \mathbf{x}_i| \leq M$ for all $i, j = 1, \dots, N$ and for all $t \geq 0$.*

In other words, in order to converge to a flock, agents should converge to a common velocity \mathbf{v}_∞ and the distance between the agents should remain uniformly bounded in time.

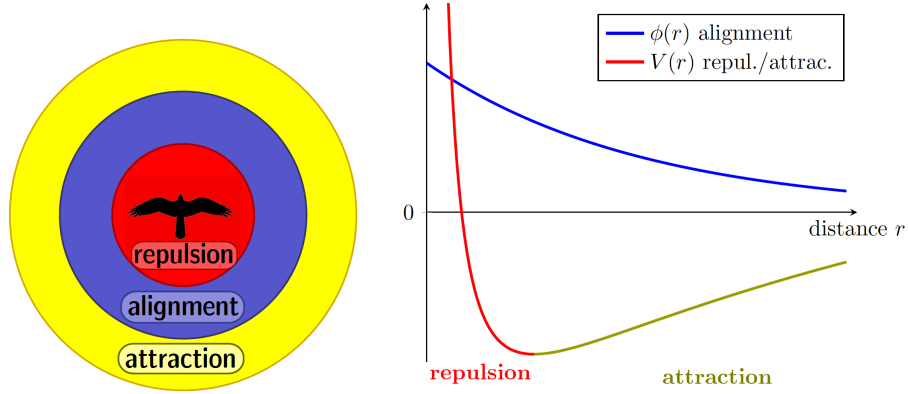


Figure 1: Left: Illustration of the three-zone model. The model includes three types of behavior: attraction, alignment and repulsion. Right: attraction and repulsions are represented through the function V , alignment is described via ϕ .

The key quantity for studying the emergence of a flock is the energy function, defined as

$$\mathcal{E}(\{\mathbf{x}_i, \mathbf{v}_i\}_i) = \frac{1}{2N} \sum_{i=1}^N |\mathbf{v}_i|^2 + \frac{1}{2N^2} \sum_{i \neq j}^N V(|\mathbf{x}_j - \mathbf{x}_i|). \quad (3)$$

We can interpret this value as the sum of the kinetic and potential energy of the system.

By itself, the attraction repulsion term (1)-(2) describes a Hamiltonian system and therefore preserves the total energy \mathcal{E} . However, the alignment term causes the total energy to decay with time. That is, it plays the role of a ‘friction term’, making the system dissipative. More precisely, we can estimate the decay rate of the energy \mathcal{E} .

Lemma 2.1. *Let $\{\mathbf{x}_i, \mathbf{v}_i\}_i$ be the solution of the N -agent system (1)(2). Then the energy \mathcal{E} (3) satisfies:*

$$\frac{d}{dt} \mathcal{E}(\{\mathbf{x}_i, \mathbf{v}_i\}_i) = -\frac{1}{2N^2} \sum_{i,j=1}^N \phi_{ij} |\mathbf{v}_j - \mathbf{v}_i|^2. \quad (4)$$

Since ϕ is a positive function, the energy \mathcal{E} is decaying along the solution trajectory.

Proof. Taking the derivative in time of the energy leads to:

$$\begin{aligned} \frac{d}{dt} \mathcal{E}(\{\mathbf{x}_i, \mathbf{v}_i\}_i) &= \frac{1}{N} \sum_{i=1}^N \dot{\mathbf{v}}_i \cdot \mathbf{v}_i + \frac{1}{2N^2} \sum_{i \neq j}^N \nabla_{\mathbf{x}_i} V(|\mathbf{x}_j - \mathbf{x}_i|) \cdot (\mathbf{v}_j - \mathbf{v}_i) \\ &= \frac{1}{N^2} \sum_{i=1}^N \sum_{j \neq i}^N (\nabla_{\mathbf{x}_i} V(|\mathbf{x}_j - \mathbf{x}_i|) \cdot \mathbf{v}_i + \phi_{ij} (\mathbf{v}_j - \mathbf{v}_i) \cdot \mathbf{v}_i) \\ &\quad + \frac{1}{2N^2} \sum_{i \neq j}^N \nabla_{\mathbf{x}_i} V(|\mathbf{x}_j - \mathbf{x}_i|) \cdot (\mathbf{v}_j - \mathbf{v}_i). \end{aligned}$$

By argument of symmetry, we find

$$\begin{aligned}
\sum_{i \neq j} \nabla_{\mathbf{x}_i} V(|\mathbf{x}_j - \mathbf{x}_i|) \cdot \mathbf{v}_i &= \sum_{i \neq j} V'(|\mathbf{x}_j - \mathbf{x}_i|) \frac{\mathbf{x}_j - \mathbf{x}_i}{|\mathbf{x}_j - \mathbf{x}_i|} \cdot \mathbf{v}_i \\
&= - \sum_{i \neq j} V'(|\mathbf{x}_j - \mathbf{x}_i|) \frac{\mathbf{x}_j - \mathbf{x}_i}{|\mathbf{x}_j - \mathbf{x}_i|} \cdot \mathbf{v}_j \\
&= \frac{1}{2} \sum_{i \neq j} V'(|\mathbf{x}_j - \mathbf{x}_i|) \frac{\mathbf{x}_j - \mathbf{x}_i}{|\mathbf{x}_j - \mathbf{x}_i|} \cdot (\mathbf{v}_i - \mathbf{v}_j).
\end{aligned}$$

Therefore we can simplify:

$$\frac{d}{dt} \mathcal{E}(\{\mathbf{x}_i, \mathbf{v}_i\}_i) = \frac{1}{N^2} \sum_{i \neq j} \phi_{ij} (\mathbf{v}_j - \mathbf{v}_i) \cdot \mathbf{v}_i$$

And so using the symmetry $\phi_{ij} = \phi_{ji}$ we conclude

$$\frac{d}{dt} \mathcal{E} = \frac{1}{2N^2} \sum_{i,j=1}^N \phi_{ij} (\mathbf{v}_j - \mathbf{v}_i) \cdot (\mathbf{v}_i - \mathbf{v}_j) = -\frac{1}{2N^2} \sum_{i,j=1}^N \phi_{ij} |\mathbf{v}_j - \mathbf{v}_i|^2.$$

□

Since the energy \mathcal{E} is decaying, we deduce that the potential energy is bounded uniformly.

Lemma 2.2. *Take $\{\mathbf{x}_i, \mathbf{v}_i\}_i$ to be a solution of the three-zone model (1)(2). There exists C such that for any time $t \geq 0$ and i, j :*

$$\sum_{i \neq j} V(|\mathbf{x}_j(t) - \mathbf{x}_i(t)|) \leq C. \quad (5)$$

Proof. Take $C_0 = \mathcal{E}(\{\mathbf{x}_i(0), \mathbf{v}_i(0)\}_i)$. Since \mathcal{E} is decaying along the solution trajectory, we deduce that for all t :

$$\frac{1}{2N} \sum_{i=1}^N |\mathbf{v}_i(t)|^2 + \frac{1}{2N^2} \sum_{i \neq j} V(|\mathbf{x}_j(t) - \mathbf{x}_i(t)|) \leq C_0$$

Since the kinetic energy $\frac{1}{2} \sum_{i=1}^N |\mathbf{v}_i|^2$ is always positive, we deduce:

$$\sum_{i \neq j} V(|\mathbf{x}_j(t) - \mathbf{x}_i(t)|) \leq 2C_0 N^2.$$

Thus taking $C = 2C_0 N^2$ yields the results. □

Taking advantage of lemma 2.2, we suppose that V is a *confinement* potential ([7]):

$$V(r) \xrightarrow{r \rightarrow \infty} +\infty \quad (6)$$

Under this assumption, we can prove the second condition of convergence to a flock, namely that the distances between agents remains bounded.

Lemma 2.3. *Suppose that V satisfies (6). Then there exists r_M such that:*

$$|\mathbf{x}_j(t) - \mathbf{x}_i(t)| \leq r_M \quad \text{for any } i, j \text{ and } t \geq 0. \quad (7)$$

Proof. From lemma 2.2, we know that the potential energy is bounded, in particular

$$V(|\mathbf{x}_j(t) - \mathbf{x}_i(t)|) \leq C$$

Since V satisfies (6), we deduce that there exists r_M such that $V(r) > C$ whenever $r > r_M$. Since $V(|\mathbf{x}_j(t) - \mathbf{x}_i(t)|)$ is bounded by C , we conclude that $|\mathbf{x}_j(t) - \mathbf{x}_i(t)|$ is bounded by r_M . \square

Remark 2.4. *Similarly, if we suppose that V diverges at $r = 0$, then there exists a minimal distance r_m between agents with*

$$|\mathbf{x}_j(t) - \mathbf{x}_i(t)| \geq r_m.$$

We can now conclude by deriving sufficient conditions to guarantee flocking behavior for the three-zone model.

Theorem 2.5. *Suppose V satisfies (6) and ϕ is strictly positive. Then for any initial condition $\{\mathbf{x}_i(0), \mathbf{v}_i(0)\}_i$ the three-zone model converges to a flock.*

Proof. Using lemma 2.3, we know that the distance between the agents remains bounded, with $|\mathbf{x}_j(t) - \mathbf{x}_i(t)| \leq r_M$. Since r_M is finite, we can take the minimum distance of ϕ on this interval:

$$m := \min_{s \in [0, r_M]} \phi(s).$$

Since ϕ is strictly positive, we deduce that $m > 0$. Therefore,

$$\phi_{ij} = \phi(|\mathbf{x}_j(t) - \mathbf{x}_i(t)|) \geq m > 0.$$

Since the energy \mathcal{E} is decaying and bounded from below we deduce that $\frac{d}{dt} \mathcal{E} \xrightarrow{t \rightarrow \infty} 0$ (as $\frac{d}{dt} \mathcal{E}$ is uniformly continuous). Therefore using lemma 2.1, we have

$$\phi_{ij} |\mathbf{v}_j - \mathbf{v}_i|^2 \xrightarrow{t \rightarrow \infty} 0.$$

Since $\phi_{ij} \geq m > 0$, we conclude that $|\mathbf{v}_j - \mathbf{v}_i| \xrightarrow{t \rightarrow \infty} 0$.

Moreover, the mean velocity $\bar{\mathbf{v}} = \frac{1}{N} \sum_i \mathbf{v}_i$ is preserved by the dynamics, by symmetry, thus

$$\mathbf{v}_i(t) \xrightarrow{t \rightarrow \infty} \bar{\mathbf{v}} \quad \text{for all } i$$

which concludes the proof. \square

2.4 Numerical investigation

To illustrate theorem 2.5, we perform numerical experiments for various choices of attraction-repulsion potentials. While theorem 2.5 guarantees that the velocities of the agents will converge to a single value, namely the mean initial value, the result does not say anything about the spatial configuration of the agents. That is, it is an open questions what *shape*

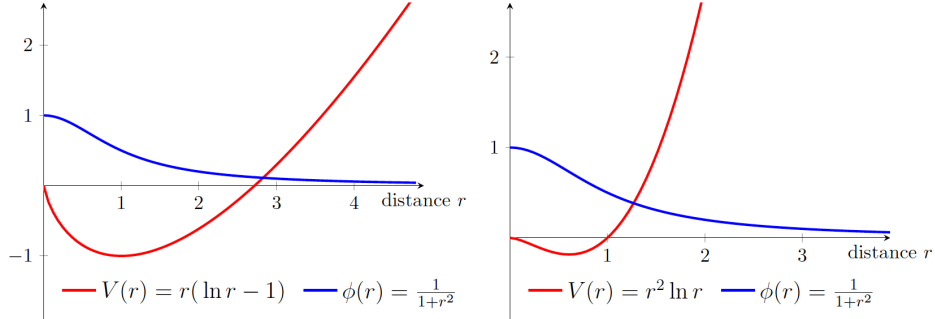


Figure 2: Attraction-repulsion V and alignment used for the simulations. In both cases, V diverges at infinity (i.e. satisfies (6))

the flock will converge to. Several previous works have studied the stability of particular equilibrium solutions in similar dynamical systems, and several patterns have been observed, some of which can be studied in our context as well. In particular, we will attempt to understand the spatial configuration of agents as $N \rightarrow \infty$.

To illustrate theorem 2.5, we consider the following two potential functions:

$$V(r) = r(\ln r - 1), \quad \phi(r) = \frac{1}{1 + r^2}. \quad (8)$$

Clearly $V(r)$ satisfies the confinement potential condition (6) (i.e. $V(r) \xrightarrow{r \rightarrow \infty} +\infty$) and ϕ is strictly positive. Thus theorem 2.5 guarantees that with these potentials, the three-zone model will converge to a flock. Figure 2 (left) illustrates these two potentials.

We use as initial conditions a uniform distribution of agents on a square of size \sqrt{N} . Their velocity is taken from a normal distribution. In figure 3, we plot the distribution of agents after $t = 200$ time units for four different group sizes: $N = 20, 50, 100$ and 1000 . For each group size, the agents regroup on a disc of radius close to 2 space units and the distribution is uniform on the disc. As the number of agents N increases, the radius remains constant and therefore the average distance between agents decreases. This type of pattern has been called *catastrophic*, since the density will eventually become singular as $N \rightarrow \infty$, and thus there is no *thermodynamic* limit. In other words, the repulsion is not strong enough to push back nearby agents.

In our second illustration, we reduce even further the repulsion force among agents using the following potential (see figure 2 (right)):

$$V(r) = r^2 \ln r, \quad \phi(r) = \frac{1}{1 + r^2} \quad (9)$$

There are now two possible equilibrium points for attraction/repulsion at the distances $r = 1$ and $r = 0$. In figure 4, we plot the distribution of agents at time $t = 100$ for two group sizes: $N = 50$ and $N = 200$. We observe that the agents are now aggregating on a circle.

The evolution of the total energy \mathcal{E} (3) is given for all cases in figure 5. As predicted by lemma 2.1, the energy is always strictly decaying. Moreover, we observe oscillatory behavior between fast and slow decay. The reason for this behavior is the repeated *contraction-expansion* of the spatial configuration as the agents approach equilibrium. The energy is decaying faster when agents are closer since the alignment function ϕ is a

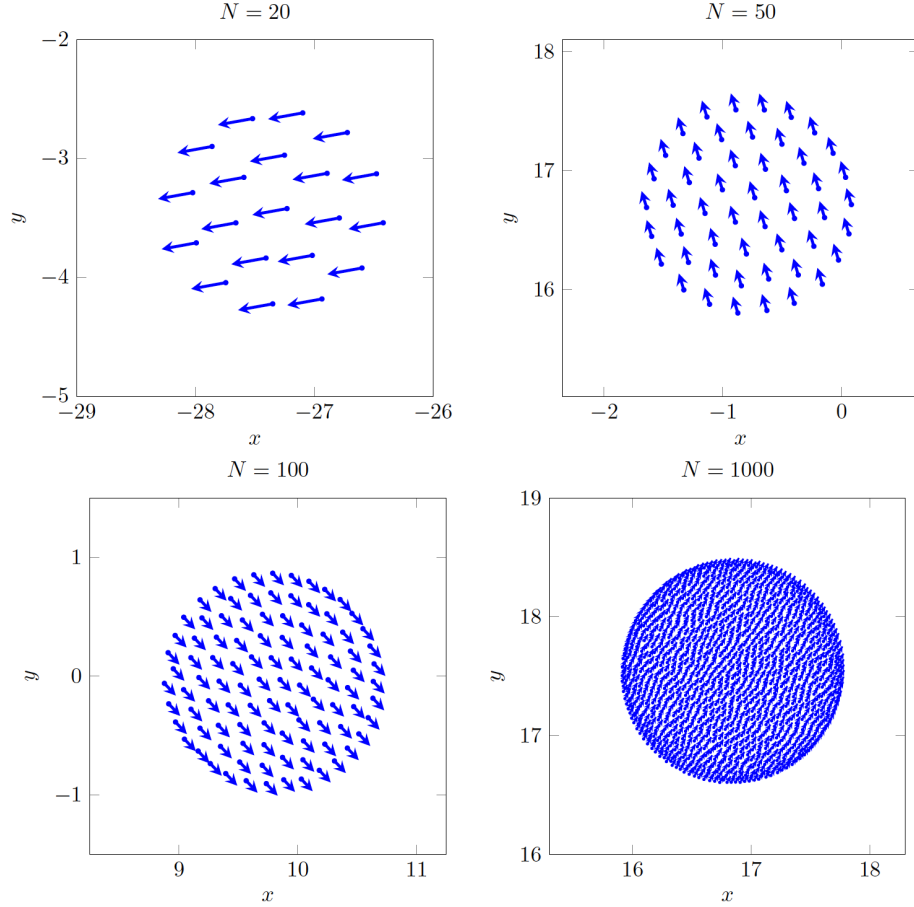


Figure 3: Simulation of the three-zone model (1)-(2) with potential V and alignment function ϕ given by (8). Agents regroup on a disc of size $R \approx 1.8$ for any group sizes. Parameters: $\Delta t = .05$, total time $T = 100$.

decaying function. These types of oscillation are also observed for the convergence of the Boltzmann equation towards global equilibrium.

2.5 Further work

In this thesis, we studied the three-zone model in the context of finitely many agents N , and derived a sufficient condition for the dynamics to converge to a flock. However, one can extend this work to the so-called *kinetic equation* associated with the particular dynamics that arises as one takes the limit $N \rightarrow \infty$. This yields an analogous partial differential equation, explicitly describing the spatial distribution of agents. While studying this equation is outside of the scope of this thesis, Motsch et. al. have derived analogous results to this work in this limiting case.

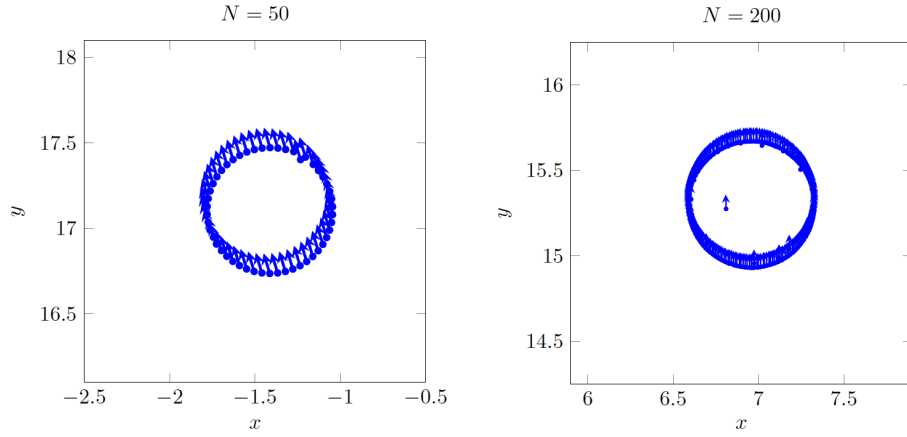


Figure 4: Simulation of the three-zone model (1)-(2) with potential V and alignment function ϕ given by (9). Agents regroup on a circle of size $R \approx .5$. Parameters: $\Delta t = .05$, total time $T = 100$.

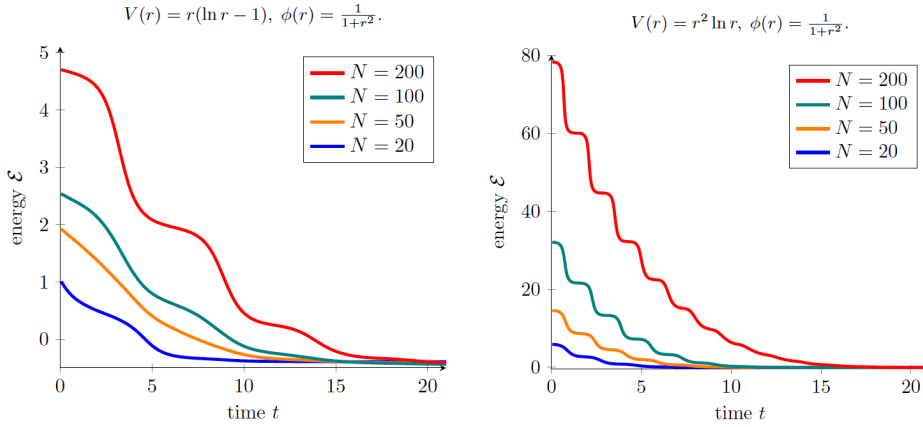


Figure 5: Evolution of the energy \mathcal{E} for the solutions depicted in figures 3 and 4. The energy is always decaying but also oscillates between fast and slow decays. These oscillations can be explained by the successive contraction-expansion of the spatial configuration. The decay of the energy is faster when the agents are closer to each other.

3 A Model of Consensus Formation on Graphs

3.1 Background

In this section, we review a deterministic model of consensus formation studied by Weber et. al. ([12]) We present the major definitions and results, though we omit proofs and intermediate lemmas for the sake of brevity. The rest of this thesis will then study a stochastic extension of this model, and as we will see, several analogous results can be obtained in this case.

Weber et. al. model opinion formation as agents interacting on a graph G , with each agent i representing a vertex and having opinion $s_i(t) \in \mathbb{R}$ at time t . The deterministic consensus model is then defined as:

Definition 3.1. *Given a collection of N agents, let $s_i \in \mathbb{R}$ represent the opinion of the i th agent. The **consensus model** is defined by the dynamics:*

$$s'_i = \sum_{j \neq i} a_{ij}(s_j - s_i) \quad \text{where} \quad a_{ij} \geq 0 \quad (10)$$

In vector notation this can be written

$$\dot{\mathbf{s}} = -L^T \mathbf{s}, \quad (11)$$

where

$$\mathbf{s} = (s_1, \dots, s_N)^T,$$

and $L = (l_{ij})_{n \times n}$ where

$$l_{ij} = \begin{cases} \sum_{i \neq j} a_{ij} & \text{if } i = j \\ -a_{ij} & \text{if } i \neq j. \end{cases} \quad (12)$$

The properties of the graph G are captured by the Laplacian matrix L , where the entries l_{ij} describe the extent to which agent i is connected to agent j . If $l_{ij} = 0$, then we say that there is no edge from agent i to agent j . The notion of consensus is then defined naturally as follows.

Definition 3.2. *We say that the consensus model converges to a **consensus** if there exists $\alpha \in \mathbb{R}$ such that:*

$$\lim_{t \rightarrow \infty} \mathbf{s}(t) = \alpha \mathbf{1}, \quad (13)$$

where $\mathbf{1} = (1, 1, \dots, 1)^T$. That is, consensus is reached whenever the opinions converge to a single value.

There are several important properties of the graph G , manifest through the Laplacian L , that we will see will be important to understand the convergence behavior of the consensus model. We summarize these in the following definition.

Definition 3.3. *Let G be a graph with $L = (l_{ij})_{ij}$ the associated Laplacian. G is **undirected** if $l_{ij} = l_{ji}$ for all i, j , otherwise G is **directed**. An undirected graph G is **connected** if there is a path between any two agents i and j . A directed graph G is **weakly connected** if when considering it as an undirected graph, it is connected. A directed graph is **strongly connected** if for any agents i and j , there is a directed path of edges from i to j .*

For any directed graph G , it is possible to partition G into strongly connected components, where each component is itself a strongly connected subgraph of G . A strongly connected component $G_1 \subseteq G$ is **isolated** if there is no edge from $G \setminus G_1$ into G_1 . When G is an undirected graph, there is a convenient representation for the connectivity of G based on the second eigenvalue λ_2 of L ; namely, G is connected if and only if $\lambda_2 > 0$. λ_2 is often called the Fiedler number of the graph G .

The first results we present from Weber et. al. are for the case of strongly connected networks, in which case we get the following theorem:

Theorem 3.1. *If G is strongly connected, then the consensus model converges to a consensus. Moreover, if G is undirected (that is, L is symmetric), then we have*

$$\mathbf{s}(t) \xrightarrow{t \rightarrow \infty} \bar{s} \mathbf{1} \quad (14)$$

where $\bar{s} = \frac{1}{N} \sum_1^N s_i(0)$. Also, in this case we have for all $i = 1, \dots, N$,

$$|s_i(t) - \bar{s}| \leq C e^{-\lambda_2 t} \quad (15)$$

where λ_2 is the Fiedler number, or the second eigenvalue of the Laplacian L .

Hence we see that in the strongly connected case we are guaranteed consensus, and moreover guaranteed to converge to the initial average whenever the graph is undirected at a rate governed by the Fiedler number λ_2 .

We now present the main result in the weakly connected case.

Theorem 3.2. *The consensus model converges for any graph G , though not necessarily to a consensus; that is, there is a vector $\mathbf{s}_\infty \in \mathbb{R}^N$ such that*

$$\mathbf{s}(t) \xrightarrow{t \rightarrow \infty} \mathbf{s}_\infty. \quad (16)$$

If the graph G has at most one isolated, strongly connected component, then the consensus model converges to a consensus.

Thus we see that while the consensus model is guaranteed to converge to some vector, convergence to consensus is only guaranteed when there is at most one isolated strongly connected component of the graph G . We will see that this is also the condition when we consider the stochastic extension of this model in the following sections. The major results of this section are summarized in figure 6.

3.2 A stochastic approach to consensus formation

We now turn our attention to a stochastic “jump” model of consensus formation on graphs, analogous to the deterministic model considered above, which shares many similarities of the “voter model” studied by Aldous ([1]). In this case, instead of modeling opinion dynamics in a deterministic manner, we model interactions between agents as arrival times of a Poisson process. We use this description to derive a continuous time Markov chain describing the dynamics of consensus formation, which can be decomposed into discrete steps by deriving the so-called embedded Markov chain of the system. Under this set up, we derive similar conditions on the graph of agents that guarantees convergence to a consensus, while noting certain results that cannot be transferred from the deterministic to the stochastic setting.

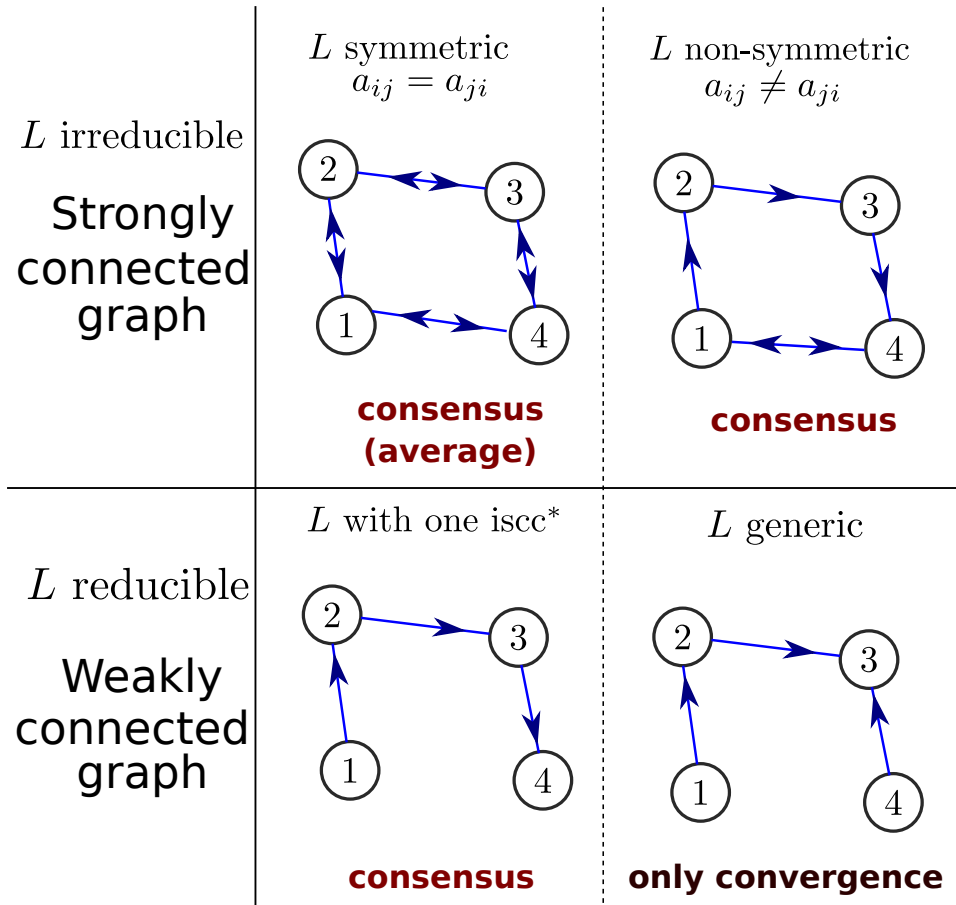


Figure 6: Summary of the results from theorems 3.1 and 3.2.

Moreover, when we make the further assumption that the underlying graph is undirected, we are able to obtain a rate of convergence that is naturally contrasted with the deterministic case considered above.

3.3 Poisson processes, interactions on graphs and the jump model

We consider a N agents, which we will denote $V = \{v_1, v_2, \dots, v_N\}$, thought of as vertices interacting on a graph, which we model as independent Poisson processes. Each agent v_i has opinion $s_i(t)$ at time $t \geq 0$, with initial opinions $s_i(0)$, $i = 1, \dots, N$. We model interactions in continuous time as a sequence of inter-arrival times: let $T_k^{(i)}$ be the time of the k^{th} interaction for agent v_i . Under the Poisson assumption, interactions satisfy the *memoryless property*, which will imply that $(T_k^{(i)})_{k \geq 1}$ are independent observations from an exponential distribution with rate parameter σ_i .

For each interaction k , v_i interacts with exactly one other agent; when agent v_i interacts with v_j , agent v_i 's opinion takes on, or “jumps” to, the value of v_j 's opinion. To denote this interaction, we define the jump function Ψ_{ij} to describe v_i interacting with v_j :

$$\Psi_{ij}(\mathbf{s}) = \mathbf{s}' \quad \text{where } s'_k = \begin{cases} s_k & \text{if } k \neq i \\ s_j & \text{if } k = i \end{cases}$$

With this in mind, we model the amount of influence agent v_i has on agent v_j as

$$p_{ij} = P(v_i \text{ interacts with } v_j \text{ at time } t | T_k^{(i)} = t),$$

which we assume is the same for all t . Then we have that v_i interacts with v_j with rate $a_{ij} = p_{ij}\sigma_i$. We can interpret the matrix $P = (p_{ij})_{i,j}$ as the edges in a weighted graph: the larger p_{ij} , the more connected v_i is to v_j , and hence the more the opinion of v_j influences that of v_i . If P is symmetric, then we say that the graph $G = (V, P)$ is *undirected*, otherwise it is *directed*. If $p_{ij} = 0$, then we say that there is no edge from v_i to v_j .

With these definitions, we can define analogous notions of connectedness to the deterministic case considered earlier.

Our primary interest is in the time evolution of the aggregate opinions

$$\mathbf{s}(t) = (s_1(t), s_2(t), \dots, s_N(t)).$$

We will see in this section that the random variable $\mathbf{s}(t)$ defines a continuous time Markov chain on the state space $S = \{(s_1, s_2, \dots, s_N) : s_i \in \{s_1(0), s_2(0), \dots, s_N(0)\} \text{ for all } i\}$. First, we recall the superposition property of Poisson processes.

Fact. [Superposition of Poisson processes] *If we have N Poisson processes with rates σ_i , we can superposition them to get a Poisson process with rate $\nu = \sum_i \sigma_i$. We call the superpositioned Poisson process $(T_n^\nu)_{n \geq 1}$.*

The Poisson process $(T_n^\nu)_n$ naturally captures the times that *any* interaction occurs. Indeed, we can use this process to describe the rate that $\mathbf{s} \in S$ transitions to any $\mathbf{s}' \in S$. We will then show that this constitutes a continuous time Markov process, which we can analyze using standard techniques.

Lemma 3.3 (Transition rates of $\mathbf{s}(t)$). *Let $\mathbf{s}, \mathbf{s}' \in S$. Then at any time t , the transition*

rates satisfy

$$a_{\mathbf{s}\mathbf{s}'} = \begin{cases} 0 & \text{if } \mathbf{s}' \text{ differs from } \mathbf{s} \text{ in more than one coordinate} \\ p_{ij}\sigma_i & \text{otherwise} \end{cases}$$

where i is the coordinate for which \mathbf{s}' differs from \mathbf{s} and v_j is the agent that v_i interacts with.

Proof. Note that for any states $\mathbf{s}, \mathbf{s}' \in S$,

$$p_{\mathbf{s}\mathbf{s}'} = P(\mathbf{s} \text{ transitions to } \mathbf{s}' \text{ at time } t \mid t = T_k^\nu, \text{ some } k) > 0$$

if and only if \mathbf{s}' differs from \mathbf{s} in at most one coordinate, otherwise $p_{\mathbf{s}\mathbf{s}'} = 0$, in which case $a_{\mathbf{s}\mathbf{s}'} = p_{\mathbf{s}\mathbf{s}'}\nu = 0$. Thus we need only consider \mathbf{s}, \mathbf{s}' that differ in a single coordinate. Then suppose that \mathbf{s}' differs from \mathbf{s} in the i^{th} coordinate. Then $s'_i = s_j$, where s_j is the j^{th} coordinate of \mathbf{s} , for some j . Then by the thinning property,

$$P(v_i \text{ interacts at time } t \mid t = T_k^\nu, \text{ some } k) = \frac{\sigma_i}{\nu}$$

Thus conditioning on this event, we have that

$$\begin{aligned} p_{\mathbf{s}\mathbf{s}'} &= P(v_i \rightarrow v_j \text{ at time } t \mid v_i \text{ interacts at time } t)P(v_i \text{ interacts at time } t \mid t = T_k^\nu, \text{ some } k) \\ &= p_{ij} \frac{\lambda_i}{\nu} \end{aligned}$$

Furthermore, the rate at which this transition occurs is $a_{\mathbf{s}\mathbf{s}'} = p_{\mathbf{s}\mathbf{s}'}\nu = p_{ij}\sigma_i$. \square

It is easy to see that $\mathbf{s}(t)$ satisfies the Markov property with transition rates $(a_{\mathbf{s}\mathbf{s}'})_{\mathbf{s}, \mathbf{s}' \in S}$, since $(T_n^\nu)_n$ are independent observations from an exponential distribution and the probabilities p_{ij} were assumed to be time independent.

Remark 3.4 (Embedded Markov chain). *We can always recover the transition probabilities from the rates given in lemma 3.3 via the identity $p_{\mathbf{s}\mathbf{s}'} = \frac{a_{\mathbf{s}\mathbf{s}'}}{\nu}$. This induces a discrete time Markov chain, called the embedded Markov chain that captures all the interactions that occur, but without any information about time. For the continuous time Markov chain $\mathbf{s}(t)$, we denote the associated embedded Markov chain $\mathbf{s}(n)$, and the transition probabilities $(p_{\mathbf{s}\mathbf{s}'})_{\mathbf{s}, \mathbf{s}' \in S}$.*

Definition 3.4 (Jump model). *Given N agents, a sequence of Poisson processes $(T_k^{(i)})_{i=1}^N$ with rates $(\sigma_i)_{i=1}^N$ and jump probabilities $P = (p_{ij})_{i,j}$, we define the jump model to be the induced continuous time Markov chain $\mathbf{s}(t)$. However, it will often be useful to use the embedded Markov chain $\mathbf{s}(n)$, which we will also refer to as the jump model.*

Note that for the jump model $\mathbf{s}(n)$, there are at most N^2 terms in the matrix $(a_{\mathbf{s}\mathbf{s}'})_{\mathbf{s}, \mathbf{s}' \in S}$ that are nonzero: given that agent v_i jumps at time n , one can interpret the distribution over which agent v_i interacts with as a distribution over actions Ψ_{ij} , where the jump Ψ_{ij} occurs with probability p_{ij} .

3.4 Convergence properties of the jump model

As we will see, many of the results of the deterministic consensus model also hold for the jump model of opinion formation. In particular, we show that, like in the deterministic

case, the connectivity of the graph $G = (V, P)$ characterizes the convergence of the opinions $\mathbf{s}(t)$. On the other hand, the stochastic nature of the jump model prevents certain results from being transferred from the deterministic setting. We begin with a simple example of this, which we will address in more detail later on.

Example 3.5 (Nonconvergence in the weakly connected case). *Consider the following three-agent setting: take $V = \{v_1, v_2, v_3\}$ with*

$$P = \begin{pmatrix} 1 & 0 & 0 \\ 0 & 1 & 0 \\ 1/2 & 1/2 & 0 \end{pmatrix}$$

Then for any initial starting state $\mathbf{s}(0) = (s_1(0), s_2(0), s_3(0))$, with $s_i(0) \neq s_j(0)$ for $i \neq j$, the jump model will never converge.

To analyze the convergence properties of the jump model $\mathbf{s}(n)$, we use the notions of *absorbing states* and *absorbing Markov chains*.

Definition 3.5 (Absorbing states and absorbing Markov chain). *Let $\mathbf{s}(n)$ be a Markov chain on a state space S . A state $\mathbf{s} \in S$ is called *absorbing* if $p_{\mathbf{s}\mathbf{s}} = 1$ – that is, the probability of staying in \mathbf{s} given that the chain has arrived in \mathbf{s} is 1. The Markov chain $\mathbf{s}(n)$ is called an *absorbing Markov chain* if for any starting state $\mathbf{s}(0) \in S$, the chain can reach an absorbing state in finitely many transitions with positive probability. A Markov chain is *absorbed* if it reaches an absorbing state.*

Absorbing Markov chains behave nicely in the following sense.

Fact. *Let $\mathbf{s}(n)$ be an absorbing Markov chain with finite state space S . Then $\mathbf{s}(n)$ is absorbed with probability 1.*

As example 3.5 illustrates, we are not guaranteed convergence of opinions in the general weakly connected case. However, using the notion of absorbing states, we will see that the same condition as in the deterministic case will guarantee convergence to consensus. We first prove the following lemma.

Lemma 3.6. *Let $\mathbf{s}(n)$ be the discrete-time jump model with transition probabilities R on the state space S . Suppose that the graph $G = (V, P)$ is weakly connected with at most 1 isolated, strongly connected component. Then let $\mathbf{s} \in S$ be any state that is not constant, so that $s_i \neq s_j$ for some i, j . Then there is a finite path $\mathbf{s}^1, \dots, \mathbf{s}^M$ occurring with positive probability so that $\mathbf{s}^1 = \mathbf{s}$, and either $s_j^M = s_i$ or $s_i^M = s_j$.*

Proof. First, assume that i and j are in the same strongly connected component. Then by definition, there is a path $i = i_1, \dots, i_M = j$ from i to j that, given that v_i jumps, occurs in M steps with probability $\prod_{k=1}^{M-1} p_{i_k i_{k+1}} > 0$. Then set $\mathbf{s}^1 = \mathbf{s}$ and $\mathbf{s}^k = \Psi_{i_k i_{k-1}}(\mathbf{s}^{k-1})$ for $k = 2, \dots, M$. Then by lemma 3.3 we have

$$p_{\mathbf{s}^k \mathbf{s}^{k+1}} = p_{i_k i_{k+1}} \frac{\sigma_{i_k}}{\nu} > 0$$

So that the probability of \mathbf{s}^1 transitioning to \mathbf{s}^M is

$$\prod_{k=1}^{M-1} p_{\mathbf{s}^k \mathbf{s}^{k+1}} > 0$$

Furthermore, since $\mathbf{s}^M = \Psi_{i_M}(\mathbf{s}^{M-1}) = \Psi_{i_j}(\mathbf{s}^{M-1})$, we have that $s_i^M = s_j$.

Now suppose that i and j are in different strongly connected components. Then by assumption, at most one of i or j is in an isolated component. Without loss of generality, assume i is in an isolated component. In this case there is a path from i to the strongly connected component of j , and then a path to j itself. Hence we can proceed as in case 1, and find a path $i \rightarrow j$ that occurs in M steps with positive probability.

Thus we have the result. \square

We will define $p_{i \rightarrow j} := \prod_{k=1}^{M-1} p_{\mathbf{s}^k \mathbf{s}^{k+1}} > 0$ as the probability of the finite path occurring in the above proof.

Theorem 3.7. *Let $\mathbf{s}(n)$ be the discrete time jump model on a graph $G = (V, P)$, with initial opinions $\mathbf{s}(0) = (s_1(0), \dots, s_N(0))$. Suppose that G is weakly connected with at most 1 isolated, strongly connected component. Then (1) the only absorbing states of $\mathbf{s}(n)$ are constant and (2) $\mathbf{s}(n)$ is an absorbing Markov chain, and therefore is absorbed with probability 1. We conclude then that $\mathbf{s}(n)$ converges to a consensus with probability 1.*

Proof. (1) Clearly constant states are absorbing, since if $\mathbf{s} \in S$ is constant, $\Psi_{ij}(\mathbf{s}) = \mathbf{s}$ for all i, j . Now suppose that $\mathbf{s} \in S$ is an absorbing state, but that $\mathbf{s} = (s_1, \dots, s_N)$ is not constant. Then there are i, j such that $s_i \neq s_j$. Then by lemma 3.6 there is a path from \mathbf{s} to $\mathbf{s}' \in S$ with $s'_j = s_i$ occurring with probability greater than 0. Hence \mathbf{s} cannot be an absorbing state, and so the only absorbing states are constant.

(2) Let $\mathbf{s}(0)$ be any starting state. First, suppose that G is strongly connected. Then let $v_{i_0} \in V$. Then by lemma 3.6, for any $v_j \in V$, there is a finite path $i_1, \dots, i_{M_{i_0j}}$ occurring with positive probability $p_{j \rightarrow i_0}$ so that $s_j^{M_{i_0j}} = s_{i_0}(0)$. Since this is true for all $v_j \in V$, $\mathbf{s}(0)$ transitions to \mathbf{s}^* where $s_j^* = s_{i_0}(0)$ for all j , in $\sum_{j \neq i_0} M_{i_0j}$ steps with probability $\prod_{j \neq i_0} p_{j \rightarrow i_0} > 0$.

Now suppose that G is not strongly connected, but has one strongly connected isolated component. Then choose $v_{i_0} \in V$ not in an isolated component. Then again using lemma 3.6 we can find a from any $v_j \in V$ to v_{i_0} , so that as above $\mathbf{s}(0)$ transitions to \mathbf{s}^* , with $s_j^* = s_{i_0}(0)$ in finitely many steps with positive probability. \square

Moreover, when the graph is undirected and connected, we have that the expected value of the consensus opinions are equal to the initial average opinion. This is analogous to the result given under the same conditions in the deterministic model.

Corollary 3.8. *Suppose G is undirected and connected. Then with probability 1, the dynamics $S(t)$ reach consensus opinion s^* at time $T < \infty$ and the consensus opinions satisfy $\mathbb{E}s^* = \frac{1}{N} \sum_1^N S(0)$.*

Proof. Let $M(t) = \sum_1^N S_i(t)$. Then $M(t)$ is a bounded martingale with at most N^2 states, and by theorem 3.7, $M(t)$ converges to $M_\infty = Ns^*$ for some consensus opinion s^* . Moreover, since the state space of $M(t)$ is finite, there exists a stopping time T that is finite with probability 1. Then by the Optional Stopping Theorem,

$$\mathbb{E}Ns^* = \mathbb{E}M_\infty = \mathbb{E}M(T) = \mathbb{E}M(0).$$

Diving by N we get

$$\mathbb{E}s^* = \frac{1}{N} \mathbb{E}M(0) = \frac{1}{N} \sum_1^N S_i(0)$$

\square

3.5 Strong convergence in the undirected case

Theorem 3.7 characterizes precisely when the opinions $\mathbf{s}(n)$ converge to a consensus. However, by considering the embedded Markov chain rather than the continuous time model $\mathbf{s}(t)$, we lose information about the rate of convergence of opinions. Recall that in the deterministic case, we were able to show that the expected variance of the opinions

$$H(\mathbf{s}(t)) = \frac{1}{N} \sum_{i=1}^N |s_i(t) - \bar{s}(t)|^2 = \frac{1}{2N^2} \sum_{i,j} |s_i(t) - s_j(t)|^2$$

is decaying in time. If one assumes that the graph $G = (V, P)$ is undirected, we obtain an analogous result for the continuous time jump model, with a rate that is naturally contrasted to that obtained in the deterministic case.

Lemma 3.9. *Suppose that the graph $G = (V, P)$ is symmetric, so that in particular $a_{ij} = a_{ji}$ for all i, j . Then the variance $H(\mathbf{s})$ decays according to*

$$\frac{d}{dt} \mathbb{E}(H(\mathbf{s})) = -\frac{1}{N^2} \mathbb{E} \left[\sum_{i,j} a_{ij} |s_j - s_i|^2 \right]$$

Proof. Conditioning on initial states, we observe from the Kolmogorov backward equations that the change in the variance satisfies

$$\frac{d}{dt} \mathbb{E}[H(\mathbf{s})] = \sum_i \sum_{j \neq i} \mathbb{E}[a_{ij}(H(\Psi_{ij}(\mathbf{s})) - H(\mathbf{s}))]$$

Moreover, the variance after observing v_i interacting with v_j is

$$H(\Psi_{ij}(\mathbf{s})) = H(\mathbf{s}) - \frac{2}{2N^2} \sum_{k=1}^N |s_k - s_i|^2 + \frac{2}{2N^2} \sum_{k=1}^N |s_j - s_k|^2 - \frac{2}{2N^2} |s_j - s_i|^2$$

From which we deduce that

$$H(\Psi_{ij}(\mathbf{s})) + H(\Psi_{ji}(\mathbf{s})) = 2H(\mathbf{s}) - \frac{4}{2N^2} |s_j - s_i|^2$$

Furthermore, exploiting the symmetry $a_{ij} = a_{ji}$ we get that

$$a_{ij}H(\Psi_{ij}(\mathbf{s})) + a_{ji}H(\Psi_{ji}(\mathbf{s})) = (a_{ij} + a_{ji}) \left[H(\mathbf{s}) - \frac{2}{2N^2} |s_j - s_i|^2 \right]$$

Thus

$$\begin{aligned} \frac{d}{dt} \mathbb{E}[H(\mathbf{s})] &= \sum_i \sum_{j \neq i} \mathbb{E}[a_{ij}(H(\Psi_{ij}(\mathbf{s})) - H(\mathbf{s}))] \\ &= \mathbb{E} \left[\sum_{i < j} (a_{ij}H(\Psi_{ij}(\mathbf{s})) + a_{ji}H(\Psi_{ji}(\mathbf{s})) - (a_{ij} + a_{ji})H(\mathbf{s})) \right] \\ &= -\frac{1}{N^2} \mathbb{E} \left[\sum_{i < j} (a_{ij} + a_{ji}) |s_j - s_i|^2 \right] = -\frac{1}{N^2} \mathbb{E} \left[\sum_{i,j} a_{ij} |s_j - s_i|^2 \right] \end{aligned}$$

□

In fact, when the graph is symmetric and strongly connected, we can obtain a similar rate of convergence as in the deterministic case. To see this, we define the matrix analogous to the Laplacian of the graph $G = (V, P)$:

$$L = \begin{bmatrix} \sigma_1 & -a_{12} & \cdots & -a_{1N} \\ -a_{21} & \sigma_2 & \ddots & \vdots \\ \vdots & \ddots & \ddots & \vdots \\ -a_{N1} & \cdots & \cdots & \sigma_N \end{bmatrix}$$

Recall that the Laplacian is positive definite, and note that since $\sigma_i = \sum_j a_{ij}$, we have for any vectors \mathbf{s}

$$(L\mathbf{s})_i = a_i s_i - \sum_{j \neq i} a_{ij} s_j = \sum_{j=1}^N a_{ij} (s_i - s_j)$$

Then clearly $\mathbf{u}_1 = (1/\sqrt{N}, 1/\sqrt{N}, \dots, 1/\sqrt{N})$ is an eigenvector with $L\mathbf{u}_1 = 0 = 0\mathbf{u}_1$, so that $\lambda_1 = 0$ is always an eigenvalue, and we have $0 = \lambda_1 \leq \lambda_2 \leq \cdots \leq \lambda_N$, for all other eigenvalues. As in the discussion in the deterministic case, the second eigenvalue, $\lambda_2 \geq 0$, called the Fiedler number, will determine the rate of convergence of the variance.

Lemma 3.10. *Let $G = (V, P)$ be symmetric and connected. Let λ_2 be the second eigenvalue of L . Then*

$$\sum_{i,j} a_{ij} |s_j - s_i|^2 \geq 2\lambda_2 N \cdot H(\mathbf{s})$$

Proof. From the above, we note that

$$\begin{aligned} \langle L\mathbf{s}, \mathbf{s} \rangle &= \sum_{i=1}^N \left(\sum_{j=1}^N a_{ij} (s_i - s_j) \right) s_i = \sum_{ij} a_{ij} (s_i - s_j) s_i \\ &= \sum_{ji} a_{ji} (s_j - s_i) s_j = \sum_{ji} a_{ij} (s_j - s_i) s_j \end{aligned}$$

where we use the fact that G is undirected, so $a_{ji} = a_{ij}$. Therefore we can write

$$\begin{aligned} \langle L\mathbf{s}, \mathbf{s} \rangle &= \frac{1}{2} \left(\sum_{ij} a_{ij} (s_j - s_i) s_j + \sum_{ij} a_{ij} (s_j - s_i) s_i \right) \\ &= \frac{1}{2} \sum_{ij} a_{ij} (s_i - s_j) (s_i - s_j) = \frac{1}{2} \sum_{ij} a_{ij} |s_i - s_j|^2 \end{aligned}$$

Moreover, since L is symmetric, we can write $D = \text{diag}(\lambda_1, \dots, \lambda_N)$ and decompose $L = UDU^T$ with U the orthogonal matrix whose columns are the eigenvectors of L . Then for

\mathbf{s} fixed, define $m = \frac{1}{N} \sum_i s_i$ and set $\bar{\mathbf{s}} = (m, m, \dots, m)^T$. Then

$$\begin{aligned}
\sum_{ij} |s_i - s_j|^2 &= \sum_{ij} |s_i - m + m - s_j|^2 \\
&= \sum_{ij} |s_i - m|^2 - 2(s_i - m)(s_j - m) + |s_j - m|^2 \\
&= 2N \sum_{ij} |s_i - m|^2 = 2N \langle \mathbf{s} - \bar{\mathbf{s}}, \mathbf{s} - \bar{\mathbf{s}} \rangle \\
&= 2N \|\mathbf{s} - \bar{\mathbf{s}}\|^2
\end{aligned}$$

Now note that $L\bar{\mathbf{s}} = 0$, so

$$\begin{aligned}
\langle L(\mathbf{s} - \bar{\mathbf{s}}), \mathbf{s} - \bar{\mathbf{s}} \rangle &= \langle L\mathbf{s}, \mathbf{s} - \bar{\mathbf{s}} \rangle \\
&= \langle L\mathbf{s}, \mathbf{s} \rangle - \langle L\mathbf{s}, \bar{\mathbf{s}} \rangle \\
&= \langle L\mathbf{s}, \mathbf{s} \rangle - \langle \mathbf{s}, L^T \bar{\mathbf{s}} \rangle \\
&= \langle L\mathbf{s}, \mathbf{s} \rangle
\end{aligned}$$

Therefore

$$\begin{aligned}
\langle L\mathbf{s}, \mathbf{s} \rangle &= \langle L(\mathbf{s} - \bar{\mathbf{s}}), \mathbf{s} - \bar{\mathbf{s}} \rangle \\
&= \langle UDU^T(\mathbf{s} - \bar{\mathbf{s}}), \mathbf{s} - \bar{\mathbf{s}} \rangle \\
&= \langle DU^T(\mathbf{s} - \bar{\mathbf{s}}), U^T(\mathbf{s} - \bar{\mathbf{s}}) \rangle
\end{aligned}$$

Then setting $\mathbf{w} = U^T(\mathbf{s} - \bar{\mathbf{s}})$, we have

$$\langle L\mathbf{s}, \mathbf{s} \rangle = \sum_i^N \lambda_i |w_i|^2$$

Notice that if we let $\mathbf{u}_1 = (1/\sqrt{N}, 1/\sqrt{N}, \dots, 1/\sqrt{N})^T$ be the first eigenvector, we have $w_1 = \langle \mathbf{u}_1, \mathbf{s} - \bar{\mathbf{s}} \rangle = 0$, from which we obtain

$$\begin{aligned}
\sum_{i=1}^N \lambda_i |w_i|^2 &= \sum_{i=2}^N \lambda_i |w_i|^2 \geq \sum_{i=2}^N \lambda_2 |w_i|^2 \\
&= \lambda_2 \sum_{i=2}^N |w_i|^2 = \lambda_2 \|\mathbf{w}\|^2 = \lambda_2 \|\mathbf{s} - \bar{\mathbf{s}}\|^2 \\
&= \lambda_2 \sum_{i=1}^N |s_i - m|^2 = \lambda_2 NH(\mathbf{s})
\end{aligned}$$

Thus

$$\sum_{ij} a_{ij} |s_j - s_i|^2 = 2 \langle L\mathbf{s}, \mathbf{s} \rangle \geq 2\lambda_2 NH(\mathbf{s}).$$

□

These lemmas give us the following theorem.

Theorem 3.11. *Let $G = (V, P)$ be symmetric and connected. Then*

$$\mathbb{E}[H(\mathbf{s}(t))] \leq e^{-\frac{2\lambda_2 t}{N}} \mathbb{E}[H(\mathbf{s}(0))]$$

Where $\lambda_2 > 0$.

Proof. From the previous lemmas we observe that

$$\frac{d}{dt} \mathbb{E}[H(\mathbf{s}(t))] = -\frac{1}{N^2} \mathbb{E}[\sum_{ij} a_{ij} |s_j - s_i|^2] \leq -\frac{2\lambda_2}{N} \mathbb{E}[H(\mathbf{s}(0))]$$

Then applying Gronwall's lemma we have,

$$\mathbb{E}[H(\mathbf{s}(t))] \leq e^{-\frac{2\lambda_2 t}{N}} \mathbb{E}[H(\mathbf{s}(0))]$$

Where $\lambda_2 > 0$ because G is connected. □

Thus we see that the variance of the opinions decays at rate $\frac{2\lambda_2}{N}$, which is naturally contrasted with the deterministic case, which we recall decayed with rate λ_2 .

3.6 Numerical investigation

We perform numerical experiments to illustrate the major results of this section, namely theorems 3.7 and 3.10. We emphasize the importance of strongly connected components of the underlying graphs, and give examples highlighting the differences between the deterministic and stochastic setting.

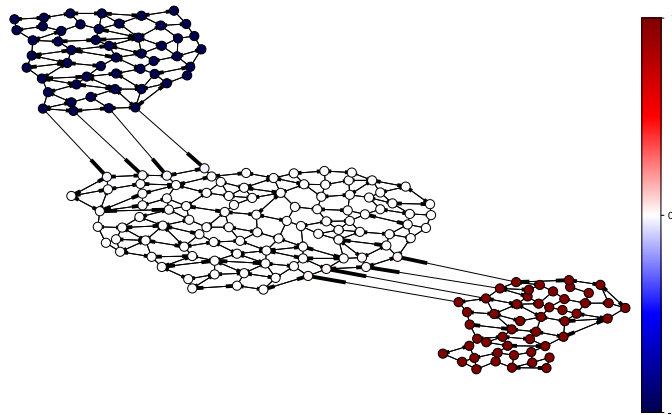


Figure 7: Illustration of the deterministic model with 2 strongly connected isolated components. Nodes in the top left component are initialized with opinion -1, whereas nodes in the bottom right component are initialized with opinion 1. Nodes in the center component are initialized with opinion 0.

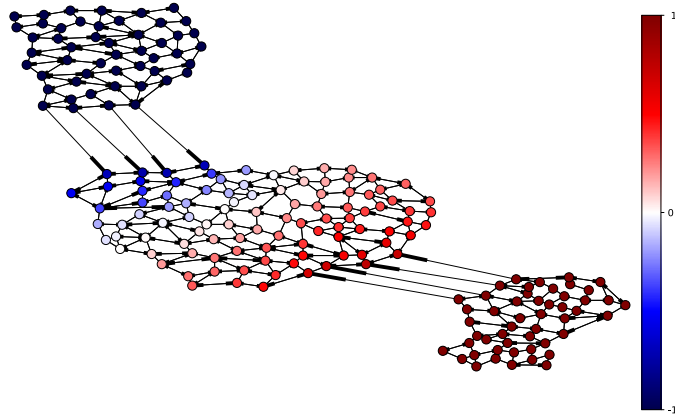


Figure 8: Illustration of the averaging effect from the deterministic consensus model with 2 strongly connected isolated components after $t=1000$ periods. By theorem 3.2, the model converges, though not to a consensus, as there is more than one isolated strongly connected component.

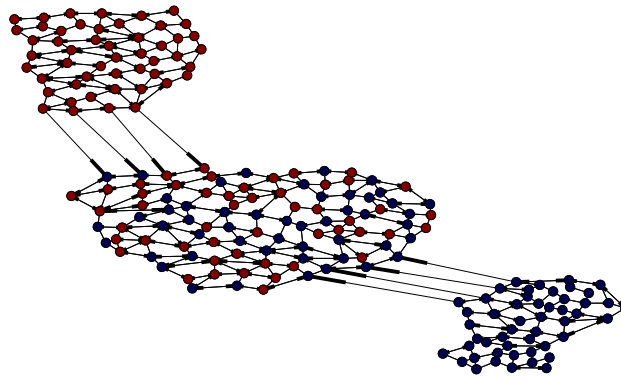


Figure 9: Illustration of the initial setup of the stochastic model with $s_i \in \{-1, 1\}$. The nodes in the bottom right connected component are initialized to have opinion 1, whereas the nodes in the top left connected component are initialized to have opinion -1. The nodes in the center component are initialized randomly with opinion -1 or 1.

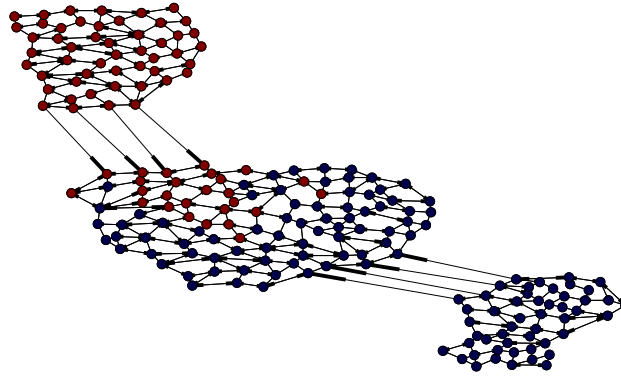


Figure 10: Stochastic consensus model after running the simulation for $t=1000$ periods. We see that the isolated components remain unchanged, and that the center component fails to reach consensus. Note that nodes more connected to the bottom right tend to have opinion 1, whereas nodes more connected to the top left component tend to have opinion -1.

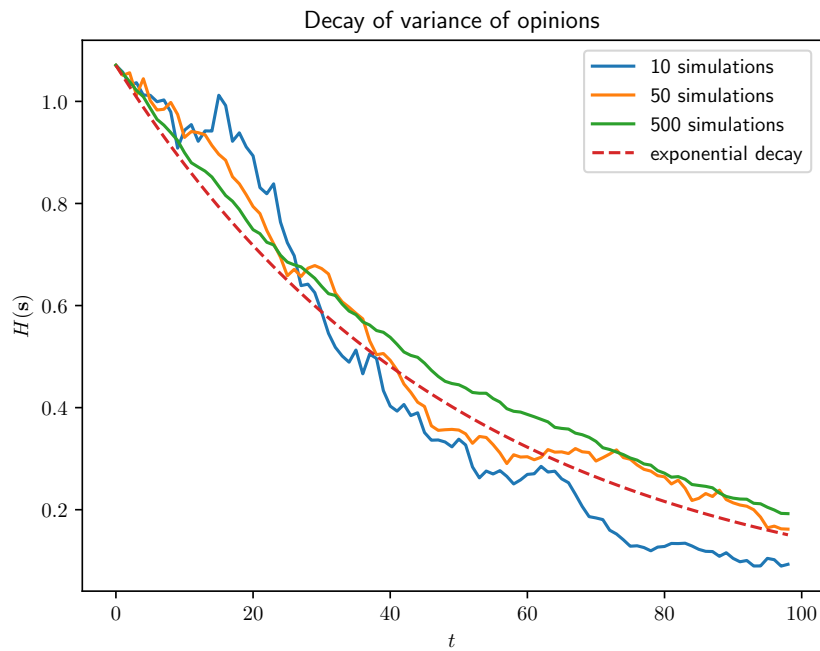


Figure 11: Illustration of the decay of variance of opinions as given by theorem 3.10, with variance averaged over 10, 50, and 500 simulations.

3.7 Further work

In this section, we briefly reviewed a deterministic model of consensus formation and proposed a stochastic extension for which we proved sufficient conditions for convergence to consensus. We noted throughout the importance of the connectivity of the underlying graph that agents interact on. An interesting extension of this problem, in the deterministic setting, is to ask, in some sense, the reverse question: given N agents with initial opinions $(s_1(0), s_2(0), \dots, s_N(0))$ and a desired value $s^* \in \mathbb{R}$, can we choose the entries l_{ij} of L to guarantee convergence to the particular value s^* ? This problem is fundamentally one of control theory, and one considered briefly in Weber et. al. We believe this question is one of both theoretical and practical interest in the context of social networks.

4 Conclusion

In this thesis, we considered two different models of interaction between N agents. In the model of flocking in three zones, we considered a model of behavior involving three forces: attraction, repulsion, and alignment, governed by the potential functions ϕ and V . We defined an energy function, which we showed decayed in time due to the ‘friction’ effect of the alignment force. This allowed us to find a sufficient condition on the potentials ϕ and V that guarantee the system’s convergence to a flock.

In the model of consensus formation, we briefly reviewed a deterministic model of consensus formation defined on a graph G . We then introduced a stochastic extension of this model, and showed that the characteristics of the graph G , in particular its connectivity, determine when the model converges to a consensus. We derived a sufficient condition for the stochastic consensus model to converge to consensus, and in the case when G is undirected, determined a rate of convergence related to the Fiedler number of the graph G .

References

- [1] David Aldous and James Allen Fill. *Reversible Markov Chains and Random Walks on Graphs*. Tech. rep. URL: <https://www.stat.berkeley.edu/~aldous/RWG/book.pdf>.
- [2] M Ballerini et al. “Interaction ruling animal collective behavior depends on topological rather than metric distance: evidence from a field study.” In: *Proceedings of the National Academy of Sciences of the United States of America* 105.4 (2008), pp. 1232–7. ISSN: 1091-6490. DOI: 10.1073/pnas.0711437105. URL: <http://www.ncbi.nlm.nih.gov/pubmed/18227508h.gov/articlerender.fcgi?artid=PMC2234121>.
- [3] Adrien Blanchet and Pierre Degond. *TOPOLOGICAL INTERACTIONS IN A BOLTZMANN-TYPE FRAMEWORK*. Tech. rep. 2015. arXiv: arXiv:1507.01099v1. URL: <https://arxiv.org/pdf/1507.01099.pdf>.
- [4] Iain D Couzin et al. “Collective memory and spatial sorting in animal groups.” In: *Journal of theoretical biology* 218.1 (2002), pp. 1–11. ISSN: 0022-5193. URL: <http://www.ncbi.nlm.nih.gov/pubmed/12297066>.
- [5] Felipe Cucker and Steve Smale. *Emergent Behavior in Flocks*. Tech. rep. 2005. URL: <http://ttic.uchicago.edu/~smale/papers/flock.pdf>.
- [6] Felipe Cucker and Steve Smale. *The Mathematics of Emergence **. Tech. rep. 2006. URL: <https://mantiq.fr/img/cucker06.pdf>.
- [7] Trygve K Karper, Antoine Mellet, and Konstantina Trivisa. *ON STRONG LOCAL ALIGNMENT IN THE KINETIC CUCKER-SMALE MODEL*. Tech. rep. URL: <https://www.math.umd.edu/~mellet/publi/KMT.pdf>.
- [8] Yue-Xian Li, Ryan Lukeman, and Leah Edelstein-Keshet. “Minimal mechanisms for school formation in self-propelled particles”. In: *Physica D* 237 (2008), pp. 699–720. DOI: 10.1016/j.physd.2007.10.009. URL: www.elsevier.com/locate/physd.
- [9] Sebastien Motsch and Eitan Tadmor. “Heterophilious Dynamics Enhances Consensus *”. In: *Society for Industrial and Applied Mathematics* 56.4 (2014), pp. 577–621. DOI: 10.1137/120901866. URL: <http://www.siam.org/journals/sirev/56-4/90186.html>.
- [10] Craig W. Reynolds et al. “Flocks, herds and schools: A distributed behavioral model”. In: *Proceedings of the 14th annual conference on Computer graphics and interactive techniques - SIGGRAPH '87*. Vol. 21. 4. New York, New York, USA: ACM Press, 1987, pp. 25–34. ISBN: 0897912276. DOI: 10.1145/37401.37406. URL: <http://portal.acm.org/citation.cfm?doid=37401.37406>.
- [11] JAMES H. VON BRECHT et al. “PREDICTING PATTERN FORMATION IN PARTICLE INTERACTIONS”. In: *Mathematical Models and Methods in Applied Sciences* 22.suppl01 (2012), p. 1140002. ISSN: 0218-2025. DOI: 10.1142/S0218202511400021. URL: <http://www.worldscientific.com/doi/abs/10.1142/S0218202511400021>.
- [12] Dylan Weber, Ryan Theisen, and Sebastien Motsch. “Deterministic versus stochastic consensus dynamics on graphs”. In: (2018).